Phloem Unloading in Sink Leaves of *Nicotiana benthamiana*: Comparison of a Fluorescent Solute with a Fluorescent Virus

Alison G. Roberts,[a] Simon Santa Cruz,[a] Ian M. Roberts,[a] Denton A. M. Prior,[a] Robert Turgeon,[b] and Karl J. Oparka[a,1]

[a] Unit of Cell Biology, Scottish Crop Research Institute, Invergowrie, Dundee DD2 5DA, United Kingdom
[b] Section of Plant Biology, Division of Biological Sciences, Cornell University, Ithaca, New York 14853

Using noninvasive imaging techniques, we compared phloem unloading of the membrane-impermeant, fluorescent solute carboxyfluorescein (CF) with that of potato virus X expressing the gene for the green fluorescent protein. Although systemic virus transport took considerably longer to occur than did CF transport, unloading of both solute and virus occurred predominantly from the class III vein network, a highly branched veinal system found between class II veins. The minor veins (classes IV and V) played no role in solute or virus import but were shown to be functional in xylem transport at the time of import by labeling with Texas Red dextran. After virus exit from the class III phloem, the minor veins eventually became infected by cell-to-cell virus movement from the mesophyll. During the sink/source transition, phloem unloading of CF was inhibited from class III veins before the cessation of phloem import through them, suggesting a symplastic isolation of the phloem in class III veins before its involvement in export. The progression of the sink/source transition for carbon was unaffected by the presence of the virus in the sink leaf. However, the virus was unable to cross the sink/source boundary for carbon that was present at the time of viral entry, suggesting a limited capacity for cell-to-cell virus movement into the apical (source) region of the leaf. A functional model of the sink/source transition in *Nicotiana benthamiana* is presented. This model provides a framework for the analysis of solute and virus movement in leaves.

INTRODUCTION

The phloem of higher plants is an essential pathway for the movement of photoassimilates from mature, exporting tissues (sources) to immature, developing tissues that exert a carbon demand (sinks) (Gifford and Evans, 1981). Classically, the mature leaf is considered a carbon source, whereas the immature leaf is viewed as a net importer of carbon (Biddulph and Cory, 1965; Dickson and Larson, 1981, 1982; Turgeon, 1989). This situation changes as the leaf matures and the sink/source transition progresses basipetally along the leaf (Larson et al., 1980; Turgeon, 1989; Fellows and Geiger, 1974). Despite frequent references in the literature to solute movement from source leaves to sink leaves, the mechanism of unloading in sink leaves has been the subject of very few studies (see Turgeon, 1989). Physiological evidence indicates a symplastic unloading pathway in tobacco (Turgeon, 1987, 1989) and sugar beet (Schmalstig and Geiger, 1985, 1987), whereas in maize, anatomical evidence favors an apoplastic unloading pathway (Evert and Russin, 1993). To date, physiological studies of unloading in sink tissues have been hindered by a lack of noninvasive techniques for discriminating the site of unloading from sub-

sequent postphloem transport (Oparka, 1990; Fisher and Oparka, 1996).

Most plant viruses also have the capacity to move over long distances in the phloem (reviewed in Maule, 1991; Leisner and Turgeon, 1993; Lucas and Gilbertson, 1994; Carrington et al., 1996; Gilbertson and Lucas, 1996), although exactly how and where such viruses exit the phloem in sink tissues remain unknown because of the lack of suitable markers for the presence of replicating virus (Gilbertson and Lucas, 1996). Also, it appears that in leaves undergoing the sink/source transition, virus movement into the apical (source) region of a developing leaf is restricted (e.g., Leisner et al., 1992, 1993), although this phenomenon has seldom been studied. In solute transport studies, the use of radioactive tracers (e.g., Biddulph and Cory, 1965; Dickson and Larson, 1981; Blechschmidt-Schneider and Eschrich, 1985; Schmalstig and Geiger, 1985, 1987; Turgeon, 1987) and fluorescent probes (Peterson and Currier, 1969; Grignon et al., 1989; Oparka et al., 1994; Wang and Fisher, 1994; Wang et al., 1994; Wright et al., 1996) has contributed significantly to the study of phloem transport, but such tools have not been previously available for studies of virus movement. In systemically infected leaves, the presence of visible symptoms, such as chlorosis or necrosis, usually indicates the presence

---

[1] To whom correspondence should be addressed. E-mail kopark@scri.sari.ac.uk; fax 44-1382-562426.

of virus. However, visible symptoms do not reveal the initial sites of phloem unloading, and symptoms may develop some time after infection has occurred. More accurate methods of localizing virus-infected cells include in situ techniques for detection of either viral RNA or virus-encoded proteins (Leisner et al., 1992, 1993). An alternative approach has been to introduce the *uidA* gene, encoding the reporter protein β-glucuronidase, into the viral genome, allowing the histochemical localization of virus-infected cells (Chapman et al., 1992; Dolja et al., 1992; see Carrington, 1996). However, both in situ hybridization and histochemical staining are invasive and do not allow for real-time studies of virus movement.

Recently, two methodological advances have made possible a direct comparison of the movement of solutes and viruses in the plant. First, it has been shown that phloem transport and unloading can be imaged within intact plants by using a confocal laser scanning microscope (CLSM; Oparka et al., 1994; Wright et al., 1996). Although currently such studies have been restricted to small experimental systems such as the Arabidopsis seedling (Oparka et al., 1994; Wright et al., 1996), this approach potentially could be expanded to examine source/sink relationships in larger plants. Second, the introduction of the gene for the green fluorescent protein (GFP) into viral genomes (Baulcombe et al., 1995; Heinlein et al., 1995; Santa Cruz et al., 1996) has permitted the noninvasive imaging of the progression of viral infections (reviewed in Oparka et al., 1996a). For potato virus X (PVX), expression of the GFP has been used to trace the cell-to-cell movement of a virus and to examine the effects of specific gene deletions on cell-to-cell movement (Baulcombe et al., 1995; Oparka et al., 1996b). The location of GFP-expressing viruses can be imaged effectively on intact plants as well as within individual tissues by CLSM (Oparka et al., 1996a). GFP-tagged viruses clearly offer great potential for studying the unloading of plant viruses in sink leaves, but such studies have not yet been undertaken.

In this study, we compare the unloading patterns of the phloem-mobile, fluorescent probe carboxyfluorescein (CF) with PVX carrying the gfp gene. We show that in sink leaves of *Nicotiana benthamiana*, the distribution patterns of both solute and virus are determined predominantly by symplastic unloading from class III veins and that movement into vein classes IV and V (the minor veins) occurs by cell-to-cell transport through the mesophyll. Using noninvasive imaging, we also demonstrate the influence of the sink/source transition on the distribution of solute and virus.

RESULTS

Vein Classification

In *N. tabacum* leaves, five vein classes have been identified (Avery, 1933; Ding et al., 1988), and a similar vein architecture was found to occur in *N. benthamiana*. The class I vein

(the midrib) branches at intervals to form class II veins. The class II veins frequently interconnect at the leaf margins, providing a "loop" between adjacent class II veins (see also Avery, 1933). Class III veins are derived from class II veins and subdivide at regular intervals to form the class III veinal network. This vein distribution is shown diagrammatically in Figure 1A. In this study, we use the term vein "class" in preference to vein "order." The latter term implies that each successive vein from the midrib branches only once to derive the next vein order. In fact, in *Nicotiana* spp, this is not the case (see Avery, 1933; Ding et al., 1988). In *N. benthamiana*, the class II veins subdivide to form a complex class III veinal network that forms "islands" within which lie the minor veins (classes IV and V; see Figure 1B). Although subdivided into islands, the class III veins occur within ridges in the abaxial lamina and retain a similar size and cell architecture throughout the lamina (Ding et al., 1988). By contrast, the minor veins are situated within the normal thickness of the leaf lamina.

Phloem Transport of CF

When expanded source leaves were labeled with 6(5)-CF diacetate, the impermeant CF moiety was translocated in the
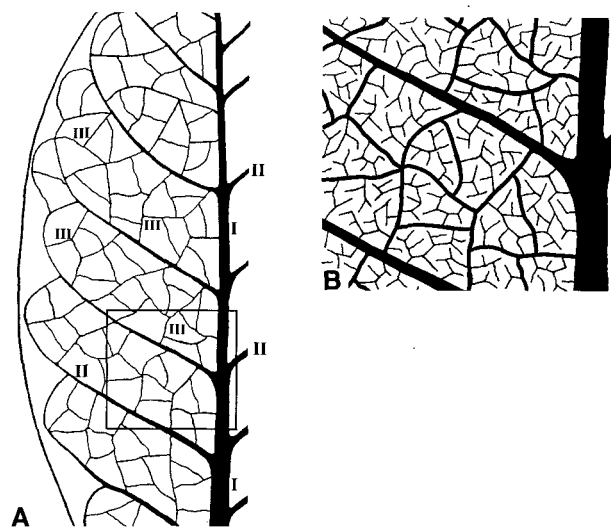
Figure 1. Diagrammatic Representation of Vein Classes in the *N. benthamiana* Leaf.

(A) The midrib (class I) gives rise at regular intervals to class II veins. The class III veinal network, a branched veinal system that forms discrete islands on the lamina, lies between the class II veins.
(B) Detail of the boxed region in **(A)** showing the position of the minor veins (classes IV and V) within the islands of the class III veinal network (adapted from Avery, 1933).

phloem to developing sink leaves (Figures 2A to 2F). The pattern of dye transport was dictated to a large extent by the phyllotaxy of the plant, with leaves directly above the labeled leaf becoming more uniformly labeled than were leaves on the opposite side of the plant. On occasion, there was an imbalance in the dye distribution on opposite sides of the same importing leaf, suggesting an uneven supply from labeled leaves below (e.g., Figure 2D). In importing leaves, phloem transport of CF was confirmed by examining petiole sections under the CLSM (Figure 2G). Occasionally, xylem transport of CF occurred. In such cases, dye transport was exceptionally rapid (<3 min), and in petiole sections, the xylem elements were labeled (data not shown).

In sink leaves displaying phloem transport of CF, dye was first seen in class I and II veins but did not spread laterally from these vein classes to the mesophyll. In contrast, after entry into the class III veinal network, CF was unloaded to the mesophyll, making the veins of the class III network look as though they were bleeding (Figures 2A to 2D and 2I). In sink leaves in which the sink/source transition was absent or had only recently commenced (e.g., Figures 2H and 2I), the class III veins and their subtending tissues became highly fluorescent with continued CF import.

Minor Veins Play No Role in Solute Unloading

In several experiments, after phloem import of CF, the leaf was detached and placed in a solution containing the 3-kD Texas Red dextran to trace xylem transport. The class IV and V veins became heavily labeled, demonstrating that the xylem but not the phloem is functional in the minor veins during the import phase. Closer examination of double-labeled leaf veins showed that although all class III veins were involved in xylem transport, parts of the class III vein network were discontinuous with respect to CF import and unloading. Such nontransporting regions appeared as unlabeled gaps in the class III network (Figures 2J and 2K). The blind endings that appeared at each end of these discontinuities were frequently sites of intense phloem unloading of CF (Figures 2A and 2B). Examination of CF-labeled class III veins at higher magnification showed that the dye had moved over considerable distances via the mesophyll after unloading (Figure 2I).

Phloem Transport of PVX Carrying the *gfp* Gene

When PVX.GFP (Baulcombe et al., 1995), which carries the *gfp* gene under the transcriptional control of a viral subgenomic promoter, was inoculated onto source leaves, fluorescent circular lesions were apparent on the lamina within 3 days postinoculation (dpi; data not shown). In the time sequence shown in Figures 3A to 3D, the infection foci on the inoculated leaf slowly increased in size as systemic symptoms developed. The first macroscopic indication of virus

entry into sink leaves was the appearance of fluorescent flecks on the lamina (Figure 3A), indicating that the virus was unloaded from discrete foci rather than uniformly along leaf veins. After the appearance of fluorescent flecks, the leaf veins became more clearly delimited by fluorescence, and with time, the mesophyll tissue between veins became labeled (Figures 3C and 3D). Fluorescent images of the first five leaves to become systemically infected are shown in Figure 3E. In sink leaves near the apex, the virus was present throughout the entire leaf, although the tips of these leaves always showed a more intense fluorescence than did the base (Figure 3E, arrows). This pattern was repeated in developing lateral leaves when they appeared (Figure 3E, lower arrows). By contrast, after the onset of the sink/source transition, the apical (source) region of the leaf showed no fluorescence, indicating the absence of virus (Figures 3C to 3E). The regions of infected leaves that showed intense GFP fluorescence went on to display chlorotic symptoms characteristic of a wild-type PVX infection (data not shown). With time, there were no discernible differences in the chlorotic symptoms (seen under natural light) between the plants infected with PVX.GFP and those infected with the wild-type virus.

Influence of Source Removal on Systemic Virus Transport

To determine the time course of a systemic infection, single mature (source) leaves on 20 plants were inoculated with the fluorescent virus PVX.GFP–CP (Santa Cruz et al., 1996), which expresses a GFP–coat protein (CP) fusion protein, and the inoculated leaves were removed at different time intervals after inoculation. The data are summarized in Figure 4. Local (fluorescent) infection sites appeared on the inoculated source leaf at 3 dpi. The first systemic symptoms (fluorescent flecks) appeared on sink leaves at ~9 dpi. Removal of source leaves later than 6 dpi had no effect on the subsequent production of systemic symptoms, suggesting that the virus had left the source leaf and was either en route to the sink leaves or already present in sink tissues at undetectable levels. Between 3 and 6 dpi, expanding fluorescent infection sites were well established on the source leaf, but removal of the source leaf during this period prevented the subsequent formation of systemic symptoms, indicating that the virus had not yet exited the inoculated leaf.

Unloading of Virus in Sink Leaves Does Not Proceed beyond Class III Veins

To identify clearly those vein classes involved in virus exit, 3-kD Texas Red dextran was introduced into the transpiration stream of detached, systemically infected leaves. Under the CLSM, the location of the Texas Red dextran was imaged
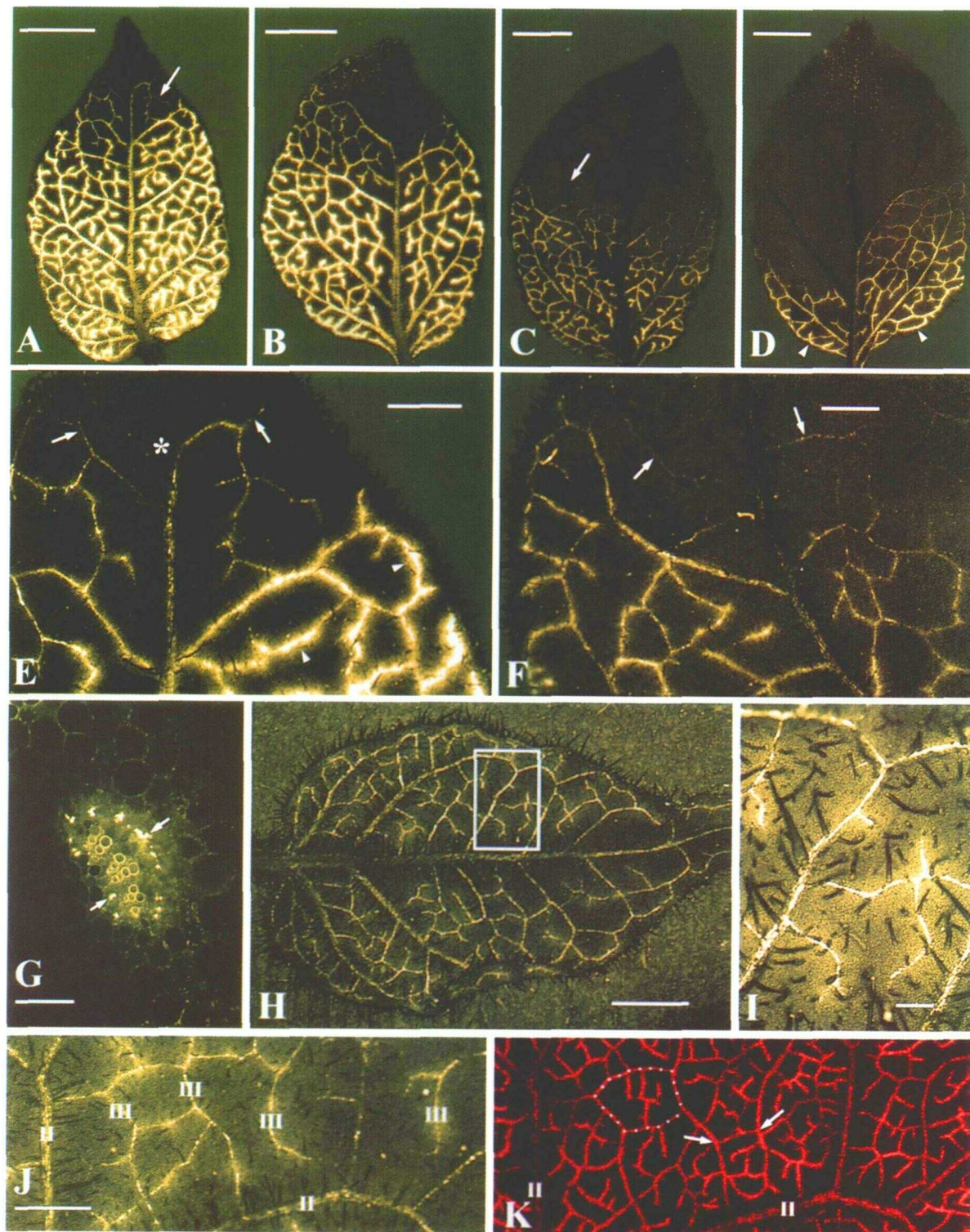
Figure 2. Noninvasive Imaging Using CLSM of Phloem Transport and Unloading of the Fluorescent Dye CF in Intact Sink Leaves of *N. benthamiana.*

separately from the GFP-tagged virus, and the two images were superimposed to reveal the sites of virus exit from the veins. By montaging several images of the leaf surface, the entire leaf could be reconstructed from the CLSM images.

In many of the leaves examined, the virus first appeared to exit the phloem at the junctions of the class III network, whereas in other cases, the virus appeared to unload along partial lengths of class III veins, that is, some distance from the class III vein junctions (Figure 3F). From the initial sites of virus unloading, the infection was observed to advance longitudinally along the vein and also in a radial direction into the mesophyll, causing the islands of the class III vein network to become more fluorescent with progressive virus unloading (Figure 3F). Frequently, the virus was found to move unidirectionally away from a class III junction, whereas the opposite side of the vein junction remained uninfected (Figure 3F, inset). Many of the fluorescent "flecks" seen macroscopically (e.g., Figure 3B) were produced by this pattern of movement. With time, several of the initial foci merged to form clearly visible "tracks" around the veins (Figure 3F). Longitudinal movement into vein classes IV and V was not observed.

The number of fluorescent foci appearing over each vein class was scored in relation to leaf development, using leaf area as an approximate indication of leaf age (Figure 5). There was considerable variability between leaves in the total number of fluorescent foci that became established on a single leaf. The number ranged from seven to 345 (data from 17 leaves). However, regardless of leaf area, virus exit occurred predominantly from class III veins (67%), with a pro-

gressive reduction in infection foci over class II (23%) and class I (10%) veins (Figure 5). There was greater variability in the distribution of foci over veins in small (<10 cm²) sink leaves, but the predominance of class III veins in virus exit was established very early in leaf development (Figure 5).

Class IV and V Veins Become Infected by Cell-to-Cell Movement from the Mesophyll

In heavily infected sink leaves, it was found that the virus eventually invades the mesophyll tissues subtended by the class III vein network (Figures 3C to 3E and inset in Figure 3F). To determine the extent to which minor veins become infected by local virus movement, areas of systemically infected leaves subtended by the class III vein network were excised for electron microscopy when fluorescent foci were first visible above class III veins (approximately at the stage shown in Figure 3F) and probed with polyclonal antibodies raised against the viral CP. A region of phloem from a class III vein, depicting plasmodesmal connections between different cell types in the bundle, is shown in Figure 6A. Serial sections of infected class III veins showed virus to be present in several cells surrounding the class III veins. In Figure 7A, virus-infected cells (identified by immunoelectron microscopy) are indicated on a light microscope image of a class III vein and surrounding tissues.

Virions were detected in several parenchyma elements surrounding the vascular elements of the class III vein but not in mature sieve elements (Figures 7A and 7C). From the

---

Figure 2. (continued).

Each whole leaf was reconstructed from several montages of overlapping regions of the leaf surface.

(A) to **(D)** Leaves undergoing the sink/source transition. The class III veinal network is labeled with CF. In **(A)** and **(B)**, the dye can be seen to unload from the class III network, particularly at blind endings, making the veins look as though they are bleeding (see also **[I]**). In the region of the sink/source transition, several of the class III veins continue to import CF but fail to unload it (arrows in **[A]** and **[C]**), giving the veins a threadlike appearance (see also **[E]** and **[F]**). In the leaf shown in **(D)**, only the most basal class III veins were still functional in unloading (small arrowheads). Bars = 0.5 cm.

(E) Enlargement of the arrowed region shown in **(A)**. Some of the veins within the class III network appear to have stopped unloading (arrows), whereas basipetal to this region, phloem unloading is still apparent (arrowheads). The asterisk indicates a point on the class I vein where CF transport ends abruptly. Bar = 1.25 mm.

(F) Enlargement of the region indicated by the arrow shown in **(C)**. In the region of the sink/source transition, faintly labeled class III veins (arrows) continue to import CF into the source region of the leaf. Bar = 1.25 mm.

(G) Transverse section of the petiole of an importing leaf. The phloem is heavily labeled with dye (arrows). Xylem vessels show autofluorescence. Bar = 200 μm.

(H) Small importing leaf showing labeling of the class III veinal network with CF. Note the functionally discontinuous nature of this vein network, with several apparent blind endings. Bar = 2 mm.

(I) Enlargement of the boxed region in **(H)**. CF is unloading from the blind endings of class III veins. Several adjoining mesophyll cells contain dye. Bar = 250 μm.

(J) and **(K)** Labeling of the class III vein network with CF and Texas Red dextran (3 kD), respectively. Portions of the class III network are indicated above individual veins (marked III). The intact leaf was imaged first for CF unloading. The leaf was then detached, and the petiole was placed subsequently in Texas Red dextran to trace xylem transport. The dotted region depicts a class III island within which lie minor veins that are functional in Texas Red but not CF transport. Arrows in **(K)** indicate bridges that sustain Texas Red but not CF transport. The position of two class II veins is also depicted (**[K]**, marked II). Bar in **(J)** = 1 mm for **(J)** and **(K)**.
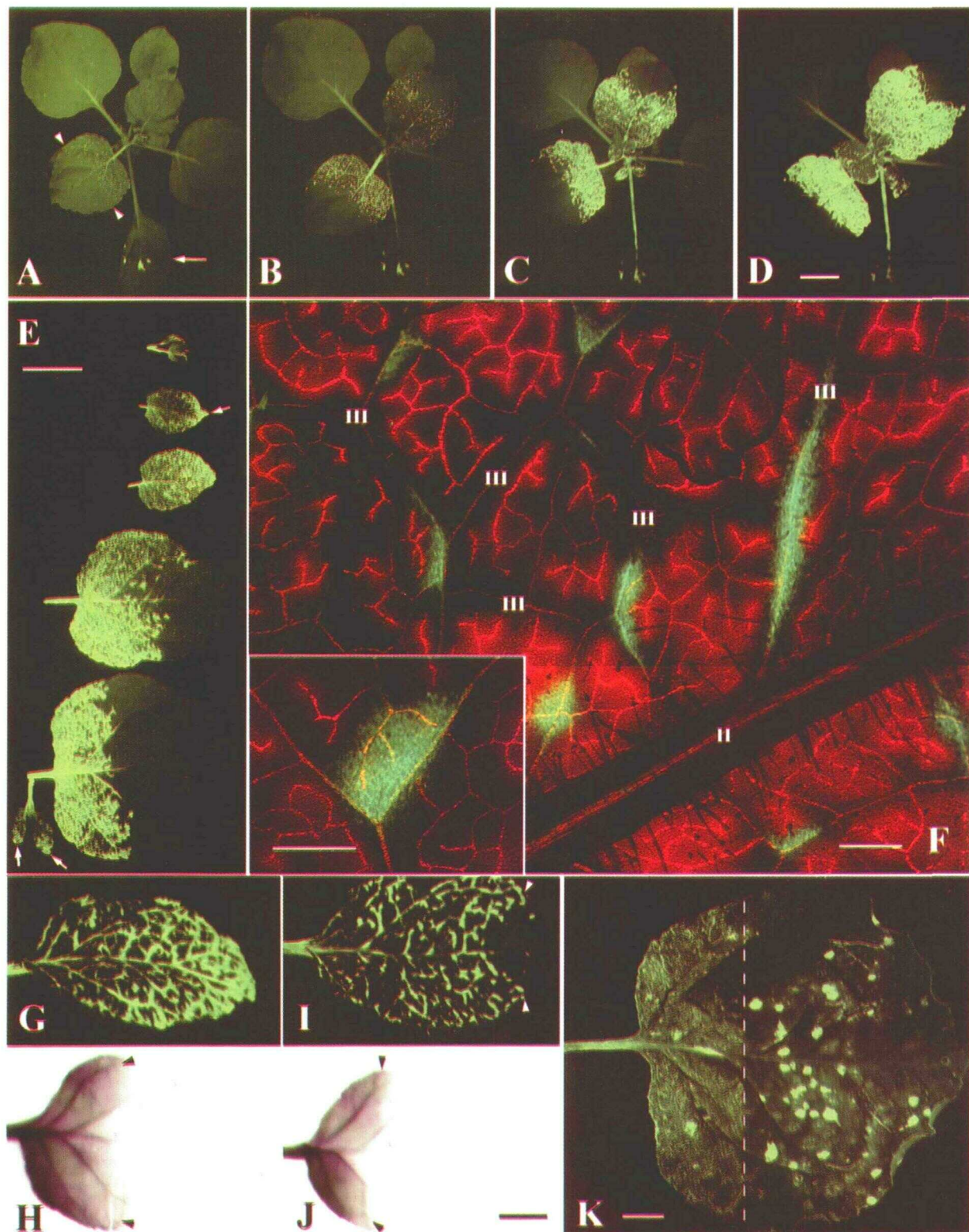
Figure 3. Systemic Movement and Unloading of PVX Expressing the Gene for the GFP (PVX.GFP).

class III vein, the virus spread laterally, infecting spongy and palisade mesophyll. Serial sections of the vein depicted in Figure 7A showed that the virus had not yet entered the epidermis. Figure 7A also shows a class IV vein. The virus was detected in the bundle sheath cells surrounding this vein, but no CP label was detected in the vascular cells within the vein, confirming observations with CF that the minor veins are not functional in import. With continued virus spread from class III veins, the minor veins eventually became infected with virus.

The class V veins of *Nicotiana* spp comprise two sieve elements, their companion cells and associated phloem parenchyma elements (Figures 6B and 6C and lower inset at center; see also B. Ding et al., 1988; X.-S. Ding et al., 1995, 1996). Infected immature and mature class V veins are shown in Figures 6B and 6C, respectively. The relative amounts of virus in the cells of a class V vein, as revealed by immunogold labeling of the viral CP, are shown schematically in the lower inset of Figure 6. In systemically infected leaves, the bundle sheath cells were heavily infected, and within the bundle sheath, vascular parenchyma elements were more heavily infected than were companion cells. Plasmodesmata were found to connect all cells of the minor vein with the bundle sheath (Figures 7B and 7C), although frequencies were not determined here. The majority of mature sieve elements showed no immunogold labeling with anti-CP antibody (Figures 7B to 7D). By contrast, immunolabeled virus aggregates were sometimes detected in the im-

mature sieve elements of class V veins, usually associated with bundles of differentiating P protein (Figures 7D and 7E).

The Sink/Source Transition

The onset of the sink/source transition in expanding leaves prevented the phloem transport of CF into the apical portion of the leaf (Figures 2A to 2D). However, in detached leaves undergoing the sink/source transition, xylem transport of Texas Red dextran into the leaf apex was unimpeded (data not shown). A consistent pattern emerged as the sink/source transition moved basipetally. In the transition zone, phloem transport continued to occur in class III veins, but unloading was no longer evident. This gave the class III veins in this region a "threadlike" appearance (e.g., arrows in Figures 2A and 2C). The transition zones of the two leaves shown in Figures 2A and 2C are shown at higher magnification in Figures 2E and 2F, respectively. Note that several class III veins close to the source region are faintly labeled, suggesting that CF continued to be imported into this region, unaccompanied by phloem unloading. In marked contrast, basipetal to the transition zone, the class III veins continued to unload CF to surrounding mesophyll tissues, as evidenced by the characteristic spread of fluorescence from these veins (Figures 2E and 2F). In the leaf shown in Figure 2D, only a small number of class III veins close to the base of the leaf were still functional in unloading.


Figure 3. (continued).

(A) to **(D)** Progression of systemic (fluorescent) symptoms in a whole plant after inoculation of a single source leaf (the inoculated leaf is marked by the arrow in **[A]**). In **(A)**, at 8 dpi, the first fluorescent foci had appeared on a sink leaf (basipetal to the arrowheads). In **(B)**, at 9 dpi, the infection foci are clearly visible as fluorescent flecks on the leaf lamina. In **(C)**, at 10 dpi, the initial foci have merged as invasion of the mesophyll progresses; the apical (source) region of leaves undergoing the sink/source transition remains uninfected. In **(D)**, at 12 dpi, the basal region of infected leaves is almost completely fluorescent. Newly developed sink leaves also show fluorescent infection symptoms. Bar in **(D)** = 2.5 cm for **(A)** to **(D)**.

(E) Detached apex and first four leaves of a systemically infected plant. In small sink leaves, the apex becomes more fluorescent than does the base (upper arrow), a feature repeated in developing lateral leaves when they appear (lower arrows). The largest two leaves shown were undergoing the sink/source transition at the time of virus entry. Bar = 2.5 cm.

(F) Unloading of virus from the class III veinal network. The virus has escaped from discrete points along class III veins and has replicated in surrounding cells. In places, the virus moves uniformly along a class III vein (to the right of image), whereas in other cases, the infection sites form fluorescent flecks (see also Figure 2B) at the junctions of class III veins. The infected leaf was allowed to transpire Texas Red dextran (see above) to highlight the minor vein network. Note the lack of virus exit from the minor veins, which are surrounded by islands of the unloading class III veins. A single class II vein is shown to the right of the image. Bar = 500 µm. The inset shows unidirectional movement from the junction of a class III vein. The virus is invading the mesophyll and minor veins subtended by a class III vein. The yellow appearance of the minor veins is a consequence of the GFP image being superimposed on the Texas Red image. It does not indicate the escape of virus from these vein classes. Bar = 500 µm.

(G) to **(J)** Infected leaves after import of carbon-14. In **(G)**, the importing leaf was a complete sink at the time of virus entry, as shown by uniform infection across the lamina. In the same leaf **(H)**, the sink/source transition for carbon, represented by carbon-14 autoradiography (arrowheads), had passed basipetally approximately two-thirds of the way along the leaf at the time of labeling. In a separate leaf on the same plant **(I)**, the sink/source transition had already commenced at the time of virus import (arrowheads). After labeling, the sink/source transition for carbon progressed almost to the base of the leaf **(J)**, again marked by arrowheads. The bar in **(J)** = 0.5 cm for **(G)** to **(J)**.

(K) Formation of local viral infection sites (fluorescent spots) on the apical (source) region of a leaf undergoing the sink/source transition at the time of inoculation. The basal region of the leaf (to the left of the dotted line) was unloading virus when the leaf was inoculated. Bar = 1 cm.
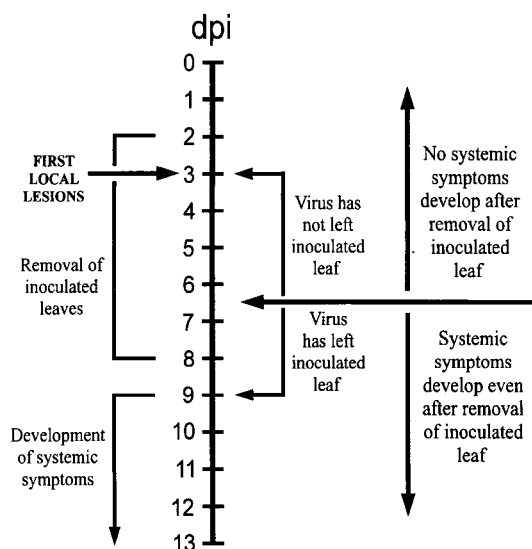
Figure 4. Diagram Showing the Time Course of a Systemic Infection after Manual Inoculation of a Single Source Leaf of *N. benthamiana* with the Virus PVX.GFP–CP.

The source leaf was removed from the plant at daily intervals between 2 and 8 dpi. Data are from 20 plants.

Viral Infection Does Not Prevent the Progression of the Sink/Source Transition

In one experiment, single mature source leaves were inoculated with PVX.GFP–CP, and fluorescent symptoms were monitored as the plant developed a systemic infection (cf. Figure 4). Twenty-four hours after the first detectable fluorescence in developing sink leaves, the same source leaf was labeled with $^{14}CO_2$, and the pattern of current–assimilate distribution was monitored by autoradiography. In the time between virus unloading and carbon-14 labeling, the sink/source transition for carbon had progressed basipetally down the sink leaves, leaving behind the sink/source boundary present at the time of virus import (Figures 3G to 3J). Thus, the normal basipetal progression of the sink/source transition was unaffected by the presence of virus in the leaf.

The Virus Is Unable to Cross the Sink/Source Boundary

In leaves undergoing the sink/source transition at the time of virus import, the virus did not subsequently invade the apical (source) region of the leaf (Figures 3B to 3E). In contrast, the virus continued to invade the mesophyll tissue in the basal region of the same leaf by cell-to-cell movement (Figures 3B to 3E). To determine whether the apical region of sink/source leaves was capable of sustaining local virus movement, this region was manually inoculated with PVX.GFP–CP after the appearance of systemic fluorescent

lesions in the lower part of the leaf. Within 3 days of this second inoculation, circular fluorescent lesions had developed on the lamina. In contrast, the basal (sink) region of the leaf continued to display the unloading pattern characteristic of sink leaves (Figure 3K). These data show that the inability of unloaded virus to spread apically into the source region of a leaf was not due to the inability of the virus to move locally in source tissues but rather to an inability to cross the sink/source boundary that was present at the time of virus entry.

DISCUSSION

N. benthamiana is host to a wide range of viruses and has been the subject of numerous investigations of host–virus interactions (Carrington et al., 1996; Gilbertson and Lucas, 1996). Despite the extensive amount of work with this plant, almost nothing is known of the pathways of solute or virus movement in developing leaves (Leisner and Turgeon, 1993; Carrington et al., 1996). Therefore, we chose this species to examine the similarities in movement between a fluorescent solute and a GFP-tagged virus in sink leaves. Our data show that PVX, although taking considerably longer to reach sink leaves by the phloem, behaves similarly to CF with respect to its unloading behavior. In *N. benthamiana,* the class II veins subdivide to give rise to a branched veinal network of class III veins that subtend the minor veins (classes IV and V; see Figure 1). These islands of class III veins appear to support the bulk of both solute and virus unloading in the leaf.
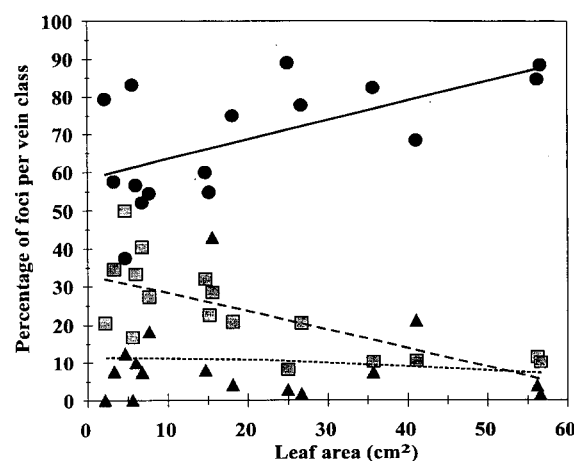
Figure 5. Appearance of the First Detectable Fluorescent Foci over Different Vein Classes in Systemically Infected Leaves after Inoculation with PVX.GFP–CP.

Values are presented as the total percentage of foci over a given vein class: ▲, class I vein; ■, class II vein; ●, class III vein). Data are derived from 1271 infection sites from 17 systemically infected leaves.
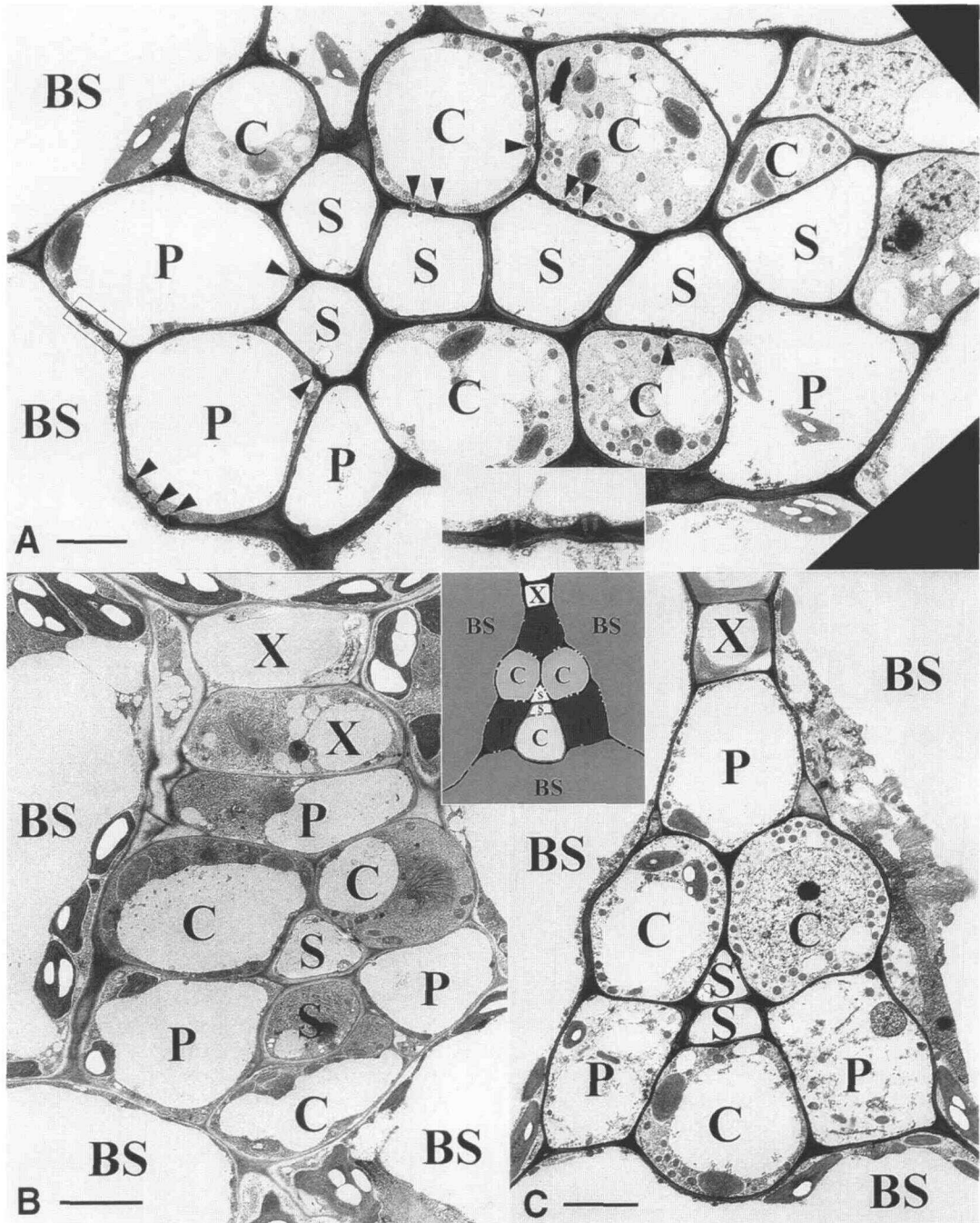
Figure 6. Ultrastructure of Leaf Veins of *N. benthamiana.*

(A) Portion of a class III vein showing plasmodesmata connecting different cell types in the phloem (arrowheads). The xylem is not shown but occurs to the right of the image. Bar = 2 μm. The inset is an enlargement of the boxed region, showing branched plasmodesmata connecting a *phloem parenchyma element* with *a bundle sheath cell.*

(B) Infected immature class V vein. Bar = 4 μm.

(C) Infected mature class V vein. The adaxial sieve element has a characteristic triangular cross-section, with two of the walls adjoining companion cells. The inset shows a diagram depicting the relative degree of viral infection of different cells in sections of class V veins after immunogold labeling of the viral CP (darker shading represents heavier infection).

BS, bundle sheath; C, companion cell; P, phloem parenchyma cell; S, sieve element; X, xylem.
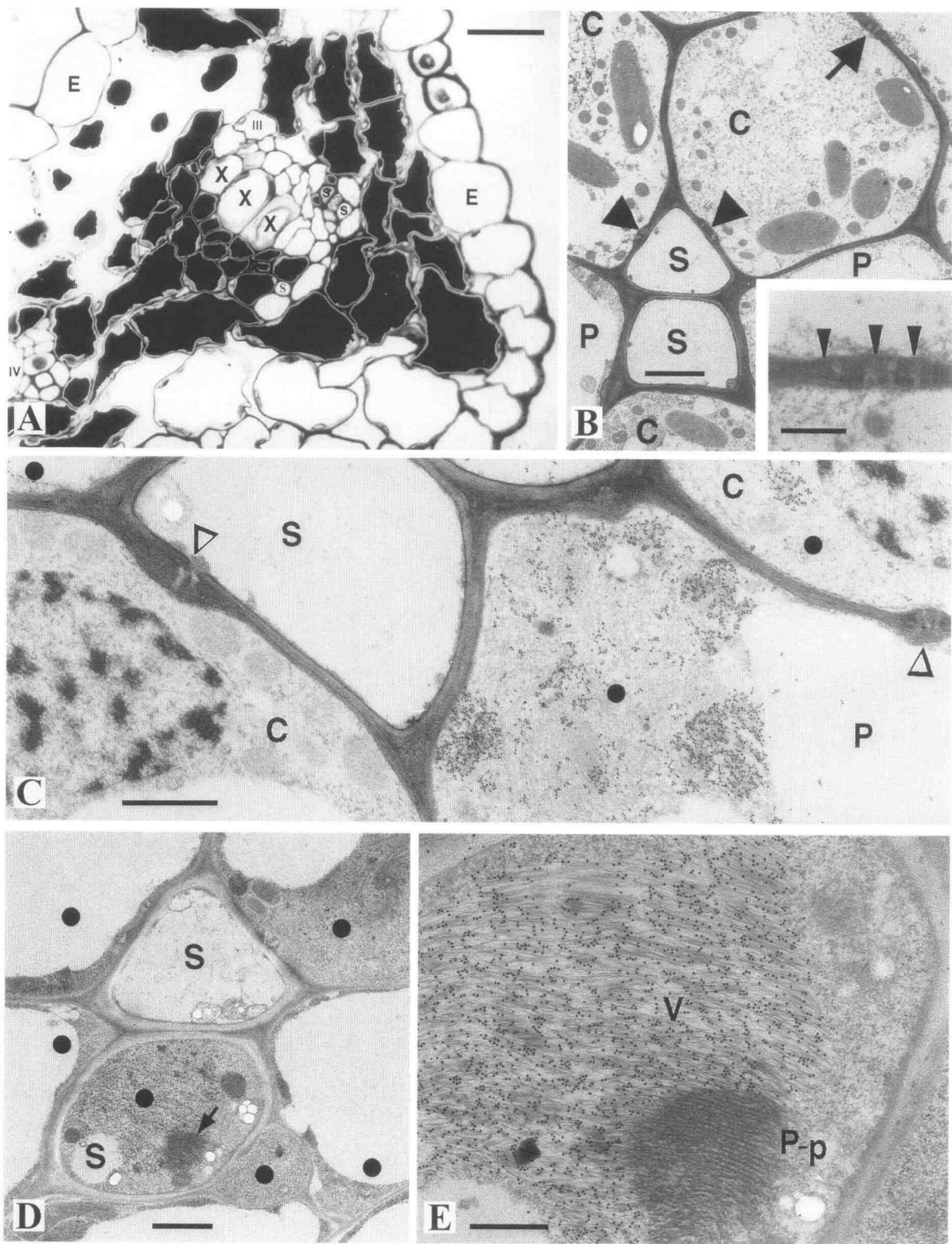
Figure 7. Immunogold Labeling of the Viral CP in Different Vein Classes.

Although the xylem of the minor veins is functional at the time of solute import, we have been unable to find any evidence that the phloem of the minor veins supports the movement of either solutes or viruses during the period of carbon import. This is consistent with autoradiographic evidence (Turgeon, 1987) and with the view that these vein classes are immature or nonfunctional at the time of import (Ding et al., 1988). Thus, phloem unloading in *N. benthamiana* is restricted predominantly to the class III veinal nework and, to a limited extent, from the lower vein classes (I and II).

Unloading of CF

Using noninvasive imaging of CF, we have been able to observe real-time events that previously have been inferred from destructive methods such as whole-leaf autoradiography (e.g., Dickson and Larson, 1981, 1982; Schmalstig and Geiger, 1985, 1987; Turgeon, 1987). Plasmodesmata were found to connect the sieve elements of the class III veins with the bundle sheath (e.g., Figure 6A), confirming a previous detailed morphometric analysis of the potential for symplastic unloading in the tobacco sink leaf (Ding et al., 1988). The reason why parts of the class III vein network are discontinuous with respect to phloem but not xylem movement is obscure. One possibility is that the phloem of this vein network is partially immature at the time of import. However, this seems unlikely because in older leaves undergoing the sink/source transition, the same discontinuous nature of CF unloading was observed. A second possibility is that these unlabeled phloem bridges are nonfunctional in phloem unloading but later are functional in phloem transport as the minor veins commence loading. These hypotheses were not tested here but deserve further study.

As the sink/source transition progressed along developing leaves, the phloem in the transition zone continued to import CF but failed to unload it. This suggests that the plasmodes-mata previously involved in symplastic phloem unloading were no longer functional. The exact interfaces at which this occurred could not be resolved, although the junction between the sieve element–companion cell (SE-CC) complex and surrounding cells is a plausible candidate. The progressive "switching off" of symplastic phloem unloading may represent a downregulation (see Lucas et al., 1993) or disappearance (Ding et al., 1988) of plasmodesmata before the involvement of class III veinal network in export. A similar progression of symplastic isolation of tissues has been observed in the Arabidopsis root tip (Duckett et al., 1994; Oparka et al., 1994). These functional demonstrations of symplastic isolation emphasize the need for caution when using plasmodesmal frequencies (plasmodesmograms) as an indicator for symplastic continuity between cell types (Van Bel and Oparka, 1995).

Unloading of Virus

In this study, PVX.GFP–CP produced fluorescent foci on sink leaves at ~9 dpi, ~1 or 2 days later than the same virus expressing GFP as a free protein (Santa Cruz et al., 1996). However, symptoms still appeared in systemically infected leaves when the inoculated leaf was removed at 6 dpi, giving a time lag of ~3 days during which the virus had exited the source leaf but was not yet visible in sink leaves. This lag phase is similar in duration to the lag period between the time of source leaf inoculation and the first detection of the fluorescent infection foci. Although both of the viruses expressing the GFP were slower to move systemically than was wild-type PVX (by 1 to 3 days), they went on to produce symptoms indistinguishable from a wild-type infection. There was no difference in the pattern of unloading obtained with either PVX.GFP or PVX.GFP–CP, although the latter virus consistently gave a more highly fluorescent signal in infected leaves. Phloem transport of current assimilate (as

---

Figure 7. (continued).

(A) Section viewed under a light microscope, indicating the distribution of infected cells (determined by immunoelectron microscopy of serial sections) around an infected class III vein. The leaf was systemically infected with PVX.GFP–CP and prepared for microscopy when fluorescent foci were first visible above class III veins (cf. Figure 3F). The virus (dark shading) has spread outward via the mesophyll but has not yet entered the epidermis. The class IV vein shown was uninfected, although bundle sheath cells surrounding it were heavily infected. Bar = 20 μm.

(B) Branched plasmodesmata connecting the adaxial sieve element of a class V vein to the two adjoining companion cells (arrowheads). Bar = 2.5 μm. The inset provides details of the region indicated by the arrow, showing branched plasmodesmata between a companion cell and bundle sheath cell. Arrowheads in the inset indicate individual plasmodesmata. Bar = 0.5 μm.

(C) Infected class V vein. Plasmodesmata connect the abaxial sieve element with its companion cell and a phloem parenchyma element with an adaxial companion cell (arrowheads). Immunogold labeling was absent from the abaxial SE-CC complex. Infected cells are indicated with filled circles. Bar = 1 μm.

(D) Part of the immature class V vein shown in Figure 6B. The adaxial SE was mature, whereas the abaxial SE was immature. The latter was heavily infected with virus. Other infected cells are indicated with filled circles. The arrow indicates an undispersed P protein body. Bar = 1 μm.

(E) Detailed view of the region indicated by the arrow in **(D)**. Assembled virus aggregates in the immature abaxial sieve element show strong immunogold localization. The virus (V) surrounds an undispersed P protein body (P-p). Bar = 1.5 μm.

C, companion cell; E, epidermis; P, phloem parenchyma; S, sieve element; X, xylem; III, class III vein; IV, class IV vein.

shown by translocation of CF) is rapid (~30 min from source to sink). Thus, the lack of viral symptoms in sink leaves was most likely attributable to replication events and/or cell-to-cell movement into and out of the phloem rather than to long-distance transport per se. The appearance of fluorescent flecks around class III veins, unlike the unloading of CF, is clearly not a real-time event. However, GFP tagging represents a considerable advance over previous, destructive methods of virus localization (Dolja et al., 1992; Leisner et al., 1992, 1993).

Despite the delay in the appearance of systemic symptoms, the class III veinal network was the principle site of unloading of PVX from the phloem. The virus did not enter the class IV and V veins via the phloem, and no fluorescent foci were associated with these vein classes, indicating a strong barrier to virus movement at the junction of class III veins with class IV veins. It is not clear how the discontinuous pattern of infection foci associated with class III veins arises. It may reflect local variations in vein anatomy, such as increased plasmodesmal densities between the phloem and surrounding mesophyll, or perhaps the ability of the plasmodesmata at these sites to be more easily modified by viral movement factor(s) to allow escape. In extensively infected leaves (e.g., Figures 3C to 3E), uniform fluorescence across the lamina was brought about by the merging of fluorescent foci along vein classes I to III followed by cell-to-cell movement between these vein classes. The exit of the virus from multiple unloading sites would reduce the amount of local virus spread required to infect the entire leaf lamina. Currently, the environmental and developmental factors influencing the number of foci forming on a sink leaf remain to be determined. However, it appears that the extent to which the leaf lamina becomes infected may be related to the total number of fluorescent foci that become established after unloading rather than to the ability of the virus to spread from cell to cell from a given infection site.

Invasion of Minor Veins

Although PVX does not enter the minor veins by phloem transport, these veins eventually become infected by local movement from the mesophyll. Plasmodesmata, although infrequent, were found to connect the sieve elements of the class V vein to the bundle sheath via the adjoining companion cells, providing a potential route for virus movement into the minor vein phloem from the mesophyll. The most likely route for such movement was from the mesophyll to the bundle sheath to the phloem parenchyma to the companion cell to the sieve element. Once inside the bundle sheath, phloem parenchyma elements became more heavily infected than companion cells. A similar situation has been observed in source leaves of tobacco plants infected with tobacco mosaic virus (Ding et al., 1995, 1996).

Although virus particles were seldom found in mature sieve elements, assembled virus aggregates were occasion-

ally found in undifferentiated sieve elements. This virus might provide a source of inoculum for the infection of new tissues once the minor veins begin to undergo loading after the sink/source transition. Thus, the sieve elements of the class V vein that become infected during the import phase may potentiate the export of virus from the leaf to new tissues when the leaf later becomes a source (see also Gilbertson and Lucas, 1996). The reason why virions were seldom detected in mature sieve elements is not known. Once in transit in the phloem, virions may become dispersed, making their detection under the electron microscope difficult. However, another possibility is that the phloem-mobile component of the virus is not in an encapsidated form but in some other infectious entity, for example, an RNA–protein complex, undetectable by immunolocalization of the viral CP.

The Sink/Source Transition Is a Barrier to Virus Movement

Once PVX has exited the phloem, it is unable to invade the apical portion of leaves undergoing the sink/source transition. This phenomenon has been noted previously but has been difficult to study without a suitable marker for virus replication. For example, similar observations of the sink/source transition were made for the movement of cauliflower mosaic virus by using a plant skeleton hybridization technique (Leisner et al., 1992, 1993). These researchers also found that phyllotaxis determines which side of a leaf the virus invades after inoculation of a single source leaf (Leisner et al., 1992). The presence of replicating PVX in infected sink leaves does not affect the progression of the sink/source transition for carbon. Thus, the presence of PVX, a virus known to induce plasmodesmal gating in various cells of the leaf (Angell et al., 1996; Oparka et al., 1996b), does not appear to interfere with the vein-loading events that ensue as the leaf becomes a source. As the sink/source transition progresses, the virus remains restricted to the basal portion of the leaf and is able to move only a limited distance across the sink/source boundary established at the time of virus entry. One explanation for the inability to invade the source region is that once unloaded from the phloem, the virus has a limited capacity to move locally from cell to cell. Thus, each infection site that becomes established on the leaf lamina may have a limited local movement capacity. The reason why local virus spread should become restricted is not yet known, although it may be related to host response mechanisms that become activated with progressive cell-to-cell movement.

A Functional Model of the Sink/Source Transition

The leaf vein classification of dicotyledonous plants is based largely on anatomical observations (e.g., Avery, 1933). The finding that the minor leaf veins of many species are the

sites of phloem loading (see Giaquinta, 1983) provided a more direct functional breakdown of leaf vein architecture. We have shown that in sink leaves of *N. benthamiana*, the class III vein network predominates in both solute and virus unloading during the import phase. The outstanding question is, "What changes occur to this vein class to allow transport out of the leaf during the export phase?" The model depicted in Figure 8 integrates the findings of this investigation with other data, including those from other species. It provides a structural and functional framework on which to base solute and virus movement studies.

According to this scheme, both solutes and virus enter the leaf by class I and II veins, respectively, but unloading does not occur from these vein classes to any great extent. The bulk of unloading occurs symplastically from the class III veinal network. In unloading tissue, both solutes and virus then enter the minor veins (classes IV and V) symplastically, but they do so from the mesophyll, not from the vascular system, because these veins are still immature. The inability of these vein classes to import either CF- or GFP-tagged viruses is most likely due to the fact that the phloem in these veins is still undifferentiated (Turgeon and Webb, 1976), although it cannot be ruled out that a symplastic discontinuity exists at the junction of the class III network with class IV veins.

In the source portion of the leaf (Figure 8, top), phloem loading begins to carry away photoassimilate. The plasmodesmata previously used in symplastic phloem unloading become downregulated, and they also diminish in number (Ding et al., 1988). At the same time, class IV and V veins mature progressively toward the finest ramifications of the vein network (Turgeon and Webb, 1976), beginning at the junction of the class III veins, which are now used for export rather than import. Because phloem loading in tobacco is apoplastic (Turgeon, 1984), development of loading capacity also involves the augmentation of sucrose carrier activity in class IV and V veins, which load the bulk of assimilates from the mesophyll. This activity is present to a limited extent in sink and source tissues, but it now becomes especially prominent in minor veins (Fellows and Geiger, 1974; Riesmeier et al., 1993; Stadler et al., 1995; Truernit and Sauer, 1995).

By the time that export has begun, symplastic continuity between the SE-CCs and surrounding cells is limited in all veins, if not eliminated altogether. As a result, diffusive efflux of sucrose from the minor vein phloem is prohibited in mature leaf tissue, and the transport system becomes unidirectional (Turgeon, 1984, 1989). Development of loading capacity in species that load symplastically has been discussed elsewhere (Turgeon, 1991).

In the above-mentioned model, it is assumed that bidirectional phloem transport (involving different sieve tubes) must occur in the class I vein, but it may also occur to a limited extent in class II and III veins within the transition zone as different minor veins begin loading at different times. It may be functionally significant that internal and external phloem bundles coexist in tobacco only as far as the class III veins but not beyond (Avery, 1933), allowing the potential for

import and export to occur in spatially separated phloem systems (see Peterson and Currier, 1969; Eschrich, 1975; Dickson and Larson, 1982).

During the symplastic import phase, turgor pressure is highest in those mature source leaves supplying a given sink leaf and lowest at the point of symplastic unloading. As the minor veins mature and begin active loading, the turgor
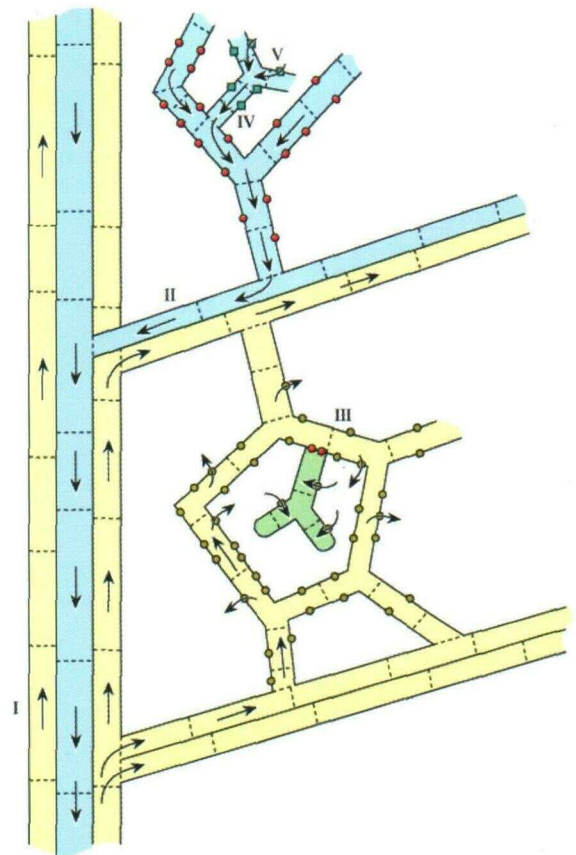
Figure 8. Schematic Model of the Sink/Source Transition in a Developing *N. benthamiana* Leaf.

At the top, the diagram depicts the exporting (source; blue) region of the leaf, and the lower part depicts the importing (sink; yellow) region of the leaf. Symplastic phloem unloading of solute and virus occurs from the class III vein network (yellow circles). In the sink portion of the leaf, the minor veins are immature (or nonfunctional; green shading) and receive assimilates (and virus) directly from the mesophyll by cell-to-cell movement. In the source portion of the leaf, the minor veins are now mature. Switching on sucrose transporters (green squares) in the minor veins signals the onset of apoplastic sucrose loading. In the source region, the class III veins function in export rather than import, which is achieved by downregulation of the plasmodesmata (red circles) that connected them to the mesophyll during the import phase. Bidirectional phloem transport (in different sieve tubes) occurs in the class I vein, but it may also occur in class II and III veins as the "transition front" passes basipetally across different vein classes.

pressure rises in these veins as a result of the sudden increase in solute levels within the SE-CC complexes. With time, the pressure gradient in the sieve tubes becomes progressively reversed as the minor veins continue to load. The reason why the class III vein plasmodesmata become nonfunctional during the export phase is not known, although one possibility is that the increase in turgor pressure brought about by continued loading induces a pressure differential between the SE-CC complex and adjoining cells sufficient to bring about plasmodesmal closure (see Oparka and Prior, 1992). The points along individual veins at which CF abruptly meets a nonfluorescent region (see, e.g., the region indicated by the asterisk in Figure 2E) are considered to represent points of equal pressure within the same sieve tubes. As an increasing number of minor veins become switched on in the source region of the leaf, this zone of equal turgor pressure progresses gradually toward the base of the leaf until the sink/source transition is complete. At the termination of the sink/source transition, the turgor pressure gradient in the phloem is completely reversed.

The above-mentioned scheme is within the realm of the original pressure flow hypothesis proposed by Münch (1930) and supported by estimates of the osmotic potential of SE-CC complexes in different vein classes of sugar beet leaves undergoing the sink/source transition (Fellows and Geiger, 1974). It now remains to be shown to what extent such a model predicts the behavior of solute and virus movement in other species with differing vein configurations. In this respect, those plants with a symplastic minor vein configuration (Van Bel, 1993; Turgeon, 1996) and that also undergo the sink/source transition (Turgeon and Webb, 1976) remain an enigma.

METHODS

Plant Material

Plants (Nicotiana benthamiana) were grown from seed in a heated glasshouse and used for experiments when they were ~20 to 30 days old.

Inoculation of Plants with Green Fluorescent Protein–Tagged Viruses

To trace the systemic movement of potato virus X (PVX), two virus constructs expressing the gene for the green fluorescent protein (GFP) were used. In the first, the GFP was expressed as a free protein (PVX.GFP; Baulcombe et al., 1995), and in the second, it was expressed as a fusion to the viral coat protein (CP) (PVX.GFP–CP; Santa Cruz et al., 1996). The construction of these viruses and their behavior in the plant have been described in detail previously (Baulcombe et al., 1995; Oparka et al., 1996b; Santa Cruz et al., 1996). Both viruses behave similarly to the wild-type virus with respect to movement (Santa Cruz et al., 1996), although PVX.GFP–CP is slower to move systemically than is either PVX or PVX.GFP in infected

N. benthamiana plants. However, in some experiments, PVX.GFP–CP was preferred to PVX.GFP because its fluorescent signal is more intense (S. Santa Cruz, unpublished data), facilitating macroscopic imaging. Source leaves were inoculated with in vitro transcripts synthesized on plasmids harboring cDNA copies of the modified viral genomes, as described previously (Chapman et al., 1992).

Imaging Intact Plants

Phloem Transport

To image phloem transport, the adaxial surface of mature source leaves was gently abraded with fine sandpaper, and ~10 μL of 6(5)-carboxyfluorescein (CF) diacetate (60 μg mL^{-1}) was applied to each leaf surface. The treated leaves were then covered with thin polythene film (Clingfilm; Merck Ltd., Poole, UK) to ensure an even coverage of dye across the leaf surface and to prevent evaporation. Importing sink leaves were examined at intervals between 10 and 30 min after labeling.

Xylem Transport

On several occasions, leaves that had imported CF were detached from the plant, and the petiole was immersed immediately in a solution containing 1 mg mL^{-1} 3-kD Texas Red dextran (Molecular Probes, Eugene, OR) to trace the xylem network in importing leaves. This size of dextran was chosen because tests with free Texas Red showed that the dye exited the xylem rapidly and stained several of the surrounding cells. Over uptake periods of ~5 to 10 min, the 3-kD Texas Red dextran remained confined predominantly to the xylem elements of the leaf.

$^{14}CO_2$ Labeling

Six systemically infected N. benthamiana plants were labeled on the same single source leaf that was used for inoculation with the virus. The plants were labeled with $^{14}CO_2$ 8 days after the source leaf was inoculated with the virus expressing the GFP as a CP fusion (PVX.GFP–CP). Each leaf received 0.37 MBq of $^{14}CO_2$ released from ^{14}C-sodium bicarbonate (ICN Radiochemicals, Irvine, CA) by addition of excess 3 M lactic acid for 30 min. After labeling, the plants were left for an additional hour to translocate carbon-14 to sink leaves. All leaves on the plant were then detached and photographed under UV illumination to reveal the pattern of GFP distribution present at the time of carbon-14 labeling (see below). The detached leaves were then pressed flat and freeze dried before autoradiography with x-ray film (RX medical film; Fuji, Tokyo, Japan) for 1 week.

Confocal Laser Scanning Microscopy

To follow the movement of CF and Texas Red dextran, an Optiphot microscope (Nikon, Tokyo, Japan) attached to a confocal laser scanning microscope (CLSM) (model MRC 1000; Bio-Rad, Hemel Hempstead, UK) system was used. To image intact plants, the microscope stage and the substage condenser of the CLSM were removed, and the intact plant, within its pot, was placed on a Perspex platform resting above the substage iris diaphragm. The upper sink leaves

were then attached to a glass plate to hold them flat and stable. In this position, the entire leaf was moved manually and viewed using low-magnification lenses (Nikon X1–X4 long working distance lenses) and blue laser excitation light (488 nm) generated from a 25-mW krypton/argon laser. To reconstruct the entire importing leaf, low-magnification images of areas of the leaf were mapped, and each image was stored individually by using the CLSM software. To subsequently reconstruct a single image of the entire leaf, the individual images were montaged using Photoshop software (Adobe, Mountain View, CA). On occasions in which detached leaves were allowed to transpire Texas Red dextran after CF import, the detached leaf was imaged first for CF by using blue (488 nm) light and immediately afterward for Texas Red dextran by using green excitation (568 nm) light. At these wavelengths, the signals from the two fluorochromes could be separated completely (see Oparka et al., 1996b). The images taken at the different wavelengths were then superimposed to reveal phloem and xylem transport on a single image of the leaf.

GFP

To detect the GFP-tagged virus, whole plants were photographed under a long-wavelength UV lamp (Blak-Ray; Ultraviolet Products Ltd., Cambridge, UK) by using Kodachrome PKL 200 daylight film. To image the progression of systemic virus infection, plants were placed on a photographic enlarger in the same position at daily intervals and photographed under UV illumination. In some experiments, after systemic virus movement, the individual leaves on a plant were detached and placed under a glass plate for UV photography. In other experiments, the infected sink leaves were removed, and the petiole was immersed in 3-kD Texas Red dextran by using the procedure described above.

Immunoelectron Microscopy

To examine the cellular distribution of the virus after its unloading from the phloem, leaf veins were first examined under the CLSM to detect the first appearance of the GFP-tagged virus. For such studies, the virus PVX.GFP–CP was used (see above). Areas of leaf veins showing the GFP were then excised with a razor blade, the tissue was fixed and embedded in resin, and sections were probed with polyclonal antibody raised against the viral CP, as described previously (Oparka et al., 1996b).

ACKNOWLEDGMENTS

REFERENCES

Angell, S.M., Davies, C., and Baulcombe, D.C. (1996). Cell-to-cell movement of potato virus X is associated with a change in the size-exclusion limit of plasmodesmata in trichome cells of *Nicotiana clevelandii*. Virology **216**, 197–201.

Avery, G.S. (1933). Structure and development of the tobacco leaf. Am. J. Bot. **20**, 565–592.

Baulcombe, D.C., Chapman, S.N., and Santa Cruz, S. (1995). Jellyfish green fluorescent protein as a reporter for virus infections. Plant J. **7**, 1045–1053.

Biddulph, O., and Cory, R. (1965). Translocation of ^{14}C metabolites in the phloem of the bean plant. Plant Physiol. **40**, 119–129.

Blechschmidt-Schneider, S., and Eschrich, W. (1985). Microautoradiographic localization of imported ^{14}C photosynthate in induced sink leaves of two dicotyledonous C_4 plants in relation to phloem unloading. Planta **163**, 439–447.

Carrington, J.C., Kasschau, K.D., Mahajan, S.K., and Schaad, M.C. (1996). Cell-to-cell and long-distance transport of viruses in plants. Plant Cell **8**, 1669–1681.

Chapman, S., Kavanagh, T., and Baulcombe, D. (1992). Potato virus X as a vector for gene expression in plants. Plant J. **2**, 549–557.

Dickson, R.E., and Larson, P.R. (1981). ^{14}C fixation, metabolic labeling patterns and translocation profiles during leaf development in *Populus deltoides*. Planta **152**, 461–470.

Dickson, R.E., and Larson, P.R. (1982). Translocation pathways in the petioles and stem between source and sink leaves of *Populus deltoides* Bartr. ex Marsh. Planta **156**, 345–358.

Ding, B., Parthasarathy, M.V., Niklas, K., and Turgeon, R. (1988). A morphometric analysis of the phloem-unloading pathway in developing tobacco leaves. Planta **176**, 307–318.

Ding, X.-S., Shintaku, M.H., Arnold, S.A., and Nelson, R.S. (1995). Accumulation of mild and severe strains of tobacco mosaic virus in minor veins of tobacco. Mol. Plant-Microbe Interact. **8**, 32–40.

Ding, X.-S., Shintaku, M.H., Crater, S.A., and Nelson, R.S. (1996). Invasion of minor veins of tobacco leaves inoculated with tobacco mosaic virus mutants defective in phloem dependent movement. Proc. Natl. Acad. Sci. USA **93**, 11155–11160.

Dolja, V.V., McBride, H.J., and Carrington, J.C. (1992). Tagging of plant potyvirus replication and movement by insertion of β-glucuronidase into the viral polyprotein. Proc. Natl. Acad. Sci. USA **89**, 10208–10212.

Duckett, C.M., Oparka, K.J., Prior, D.A.M., Dolan, L., and Roberts, K. (1994). Dye coupling in the root epidermis of *Arabidopsis* is progressively reduced during development. Development **120**, 3247–3255.

Eschrich, W. (1975). Bidirectional transport. In Encyclopedia of Plant Physiology, Vol. 1, Transport in Plants. 1. Phloem Transport, M.H. Zimmermann and J.A. Millburn, eds (Berlin: Springer-Verlag), pp. 245–255.

Evert, R.F., and Russin, W.A. (1993). Structurally, phloem unloading in the maize leaf cannot be symplastic. Am. J. Bot. **80**, 1310–1317.

Fellows, R.J., and Geiger, D.R. (1974). Structural and physiological changes in sugar beet leaves during sink to source conversion. Plant Physiol. **54**, 877–885.

Fisher, D.B., and Oparka, K.J. (1996). Post-phloem transport: Principles and problems. J. Exp. Bot. **47**, 1141–1154.

Giaquinta, R. (1983). Phloem loading of sucrose. Annu. Rev. Plant Physiol. **34**, 347–387.

Gifford, R.M., and Evans, L.T. (1981). Photosynthesis, carbon partitioning and yield. Annu. Rev. Plant Physiol. **32**, 485–509.

Gilbertson, R.L., and Lucas, W.J. (1996). How do viruses traffic on the vascular highway? Trends Plant Sci. **1**, 260–268.

Grignon, N., Touraine, B., and Durand, M. (1989). 6(5)-Carboxyfluorescein as a tracer of phloem sap translocation. Am. J. Bot. **76**, 871–877.

Heinlein, M., Epel, B.L., Padgett, H.S., and Beachy, R.N. (1995). Interaction of tobamovirus movement proteins with the plant cytoskeleton. Science **270**, 1983–1985.

Larson, P.R., Isebrands, J.G., and Dickson, R.E. (1980). Sink to source transition of *Populus* leaves. Ber. Dtsch. Bot. Ges. **93**, 79–90.

Leisner, S.M., and Turgeon, R. (1993). Movement of virus and photoassimilate in the phloem: A comparative analysis. Bioessays **15**, 741–748.

Leisner, S.M., Turgeon, R., and Howell, S.H. (1992). Long distance movement of cauliflower mosaic virus in infected turnip plants. Mol. Plant-Microbe Interact. **5**, 41–47.

Leisner, S.M., Turgeon, R., and Howell, S.H. (1993). Effects of host plant development and genetic determinants on the long-distance movement of cauliflower mosaic virus in Arabidopsis. Plant Cell **5**, 191–202.

Lucas, W.J., and Gilbertson, R.L. (1994). Plasmodesmata in relation to viral movement within leaf tissues. Annu. Rev. Phytopathol. **32**, 387–411.

Lucas, W.J., Ding, B., and Van der Schoot, C. (1993). Plasmodesmata and the supracellular nature of plants. New Phytol. **125**, 435–476.

Maule, A.J. (1991). Virus movement in infected plants. Crit. Rev. Plant Sci. **9**, 457–473.

Münch, E. (1930). Die Stoffbewegungen in der Pflanze. (Jena, Germany: G. Fischer).

Oparka, K.J. (1990). What is phloem unloading? Plant Physiol. **94**, 393–396.

Oparka, K.J., and Prior, D.A.M. (1992). Direct evidence for pressure-generated closure of plasmodesmata. Plant J. **2**, 741–750.

Oparka, K.J., Duckett, C.M., Prior, D.A.M., and Fisher, D.B. (1994). Real-time imaging of phloem unloading in the root tip of Arabidopsis. Plant J. **6**, 759–766.

Oparka, K.J., Boevink, P., and Santa Cruz, S. (1996a). Studying the movement of plant viruses using green fluorescent protein. Trends Plant Sci. **1**, 412–418.

Oparka, K.J., Roberts, A.G., Roberts, I.M., Prior, D.A.M., and Santa Cruz, S. (1996b). Viral coat protein is targeted to, but does not gate, plasmodesmata during cell-to-cell movement of potato virus X. Plant J. **10**, 805–813.

Peterson, C.A., and Currier, H.B. (1969). An investigation of bidirectional transport in the phloem. Physiol. Plant. **22**, 1238–1250.

Reismeier, J.W., Hirner, B., and Frommer, W.B. (1993). Potato sucrose transporter expression in minor veins indicates a role in phloem loading. Plant Cell **5**, 1591–1598.

Santa Cruz, S., Chapman, S., Roberts, A.G., Roberts, I.M., Prior, D.A.M., and Oparka, K.J. (1996). Assembly and movement of a plant virus carrying a green fluorescent protein overcoat. Proc. Natl. Acad. Sci. USA **93**, 6286–6290.

Schmalstig, J.G., and Geiger, D.R. (1985). Phloem unloading in developing leaves of sugar beet. I. Evidence for pathway through the symplast. Plant Physiol. **79**, 237–241.

Schmalstig, J.G., and Geiger, D.R. (1987). Phloem unloading in developing leaves of sugar beet. II. Termination of phloem unloading. Plant Physiol. **83**, 49–52.

Stadler, R., Brandner, J., Schulz, A., Gahrtz, M., and Sauer, N. (1995). Phloem loading by the PmSUC2 sucrose carrier from *Plantago major* occurs into companion cells. Plant Cell **7**, 1545–1554.

Truernit, E., and Sauer, N. (1995). The promoter of the *Arabidopsis thaliana* SUC2 sucrose-H$^+$ symporter gene directs expression of β-glucuronidase to the phloem: Evidence for phloem loading and unloading by SUC2. Planta **196**, 564–570.

Turgeon, R. (1984). Termination of nutrient import and development of vein loading capacity in albino tobacco leaves. Plant Physiol. **76**, 45–48.

Turgeon, R. (1987). Phloem unloading in tobacco sink leaves: Insensitivity to anoxia indicates a symplastic pathway. Planta **171**, 73–81.

Turgeon, R. (1989). The sink–source transition in leaves. Annu. Rev. Plant Physiol. Plant Mol. Biol. **40**, 119–138.

Turgeon, R. (1991). Symplastic phloem loading and the sink–source transition in leaves: A model. In Recent Advances in Phloem Transport and Assimilate Compartmentation, J.L. Bonnemain, S. Delrot, and W.J. Lucas, eds (Rennes, France: Ouest Editions), pp. 18–22.

Turgeon, R. (1996). Phloem loading and plasmodesmata. Trends Plant Sci. **1**, 418–423.

Turgeon, R., and Webb, J.A. (1976). Leaf development and phloem transport in *Cucurbita pepo*. Maturation of the minor veins. Planta **129**, 265–269.

Van Bel, A.J.E. (1993). Strategies of phloem loading. Annu. Rev. Plant Physiol. Plant Mol. Biol. **44**, 253–281.

Van Bel, A.J.E., and Oparka, K.J. (1995). On the validity of plasmodesmograms. Bot. Acta **108**, 174–182.

Wang, H.L., Offler, C.E., Patrick, J.W., and Ugalde, T.D. (1994). The cellular pathway of photosynthate transfer in the developing wheat grain. I. Delineation of a potential transfer pathway using fluorescent dyes. Plant Cell Environ. **17**, 257–267.

Wang, N., and Fisher, D.B. (1994). The use of fluorescent tracers to characterize the post-phloem transport pathway in maternal tissues of developing wheat grains. Plant Physiol. **104**, 17–27.

Wright, K.M., Horobin, R., and Oparka, K.J. (1996). Phloem mobility of fluorescent xenobotics in *Arabidopsis* in relation to their physicochemical properties. J. Exp. Bot. **47**, 1779–1787.

Phloem Unloading in Sink Leaves of Nicotiana benthamiana: Comparison of a Fluorescent Solute with a Fluorescent Virus

A. G. Roberts, S. S. Cruz, I. M. Roberts, DAM. Prior, R. Turgeon and K. J. Oparka

This information is current as of September 18, 2008

Permissions	https://www.copyright.com/ccc/openurl.do?sid=pd_hw1532298X&issn=1532298X&WT.mc_id=pd_hw1532298 X
eTOCs	Sign up for eTOCs for *THE PLANT CELL* at: http://www.plantcell.org/subscriptions/etoc.shtml
CiteTrack Alerts	Sign up for CiteTrack Alerts for *Plant Cell* at: http://www.plantcell.org/cgi/alerts/ctmain
Subscription Information	Subscription information for *The Plant Cell* and *Plant Physiology* is available at: http://www.aspb.org/publications/subscriptions.cfm